

QUARTERLY TECHNICAL PROGRESS REPORT  
NUMBER 10

THE ECONOMICAL PRODUCTION OF  
ALCOHOL FUELS FROM  
COAL-DERIVED SYNTHESIS GAS

CONTRACT NO. DE-AC22-91PC91034

REPORTING PERIOD:

January 1, 1994 to March 31, 1994

SUBMITTED TO:

Document Control Center  
U.S. Department of Energy  
Pittsburgh Energy Technology Center  
P.O. Box 10940, MS 921-118  
Pittsburgh, PA 15236-0940

SUBMITTED BY:

West Virginia University Research Corporation  
on behalf of West Virginia University  
213 Glenlock Hall  
Morgantown, WV 26506

April, 1994

U.S. DOE Patent Clearance is not required prior to the publication of this document.

**DISCLAIMER**

This report was prepared as an account of work sponsored by an agency of the United States Government. Neither the United States Government nor any agency thereof, nor any of their employees, makes any warranty, express or implied, or assumes any legal liability or responsibility for the accuracy, completeness, or usefulness of any information, apparatus, product, or process disclosed, or represents that its use would not infringe privately owned rights. Reference herein to any specific commercial product, process, or service by trade name, trademark, manufacturer, or otherwise does not necessarily constitute or imply its endorsement, recommendation, or favoring by the United States Government or any agency thereof. The views and opinions of authors expressed herein do not necessarily state or reflect those of the United States Government or any agency thereof.

**MASTER**

**DISTRIBUTION OF THIS DOCUMENT IS UNLIMITED**

## TABLE OF CONTENTS

Executive Summary . . . . .	1
<b>TASK 1. REACTION STUDIES . . . . .</b>	<b>3</b>
1.1 Introduction . . . . .	3
1.2 Accomplishments, Results and Discussion . . . . .	3
1.2.1 Laboratory Setup . . . . .	3
1.2.2 Molybdenum-Based Catalyst Research . . . . .	4
1.2.3 Transition-Metal-Oxide Catalyst Research . . . . .	7
1.2.4 Reaction Engineering . . . . .	7
1.3 Conclusions and Recommendations . . . . .	9
1.4 Future Plans . . . . .	10
1.5 References for Task 1 . . . . .	10
<b>TASK 2. PROCESS SYNTHESIS AND EVALUATION . . . . .</b>	<b>16</b>
2.1 Introduction . . . . .	16
2.2 Accomplishments, Results and Discussion . . . . .	16
2.2.1 Design and Optimization Of Alcohol Production, Separation and Blending . . . . .	16
2.2.1.1 Problem Definition . . . . .	16
2.2.1.2 Simulated Annealing . . . . .	17
2.2.1.3 Solution Methodology . . . . .	18
2.2.1.4 Results . . . . .	20
2.2.2 Economic Analysis . . . . .	22
2.2.2.1 Overall Efficiency . . . . .	22
2.2.2.2 Multi-Objective Model Development . . . . .	22
2.2.3 Monte Carlo Simulation of Process Uncertainties . . . . .	25
2.2.4 Fuel Testing . . . . .	27
2.2.4.1 Fuel Specifications . . . . .	27
2.2.4.2 Exhaust Gas Emissions Sampling System . . . . .	28
2.3 Conclusions and Recommendations . . . . .	28
2.4 References for Task 2 . . . . .	29

## LIST OF TABLES

Table I. Experimental Variables . . . . .	13
Table II. Mo 3d and S 2p Binding Energies . . . . .	13
Table III. Experimental Variables . . . . .	14
Table IV. Chain-Growth Reaction Scheme . . . . .	15
Table 2.1 Compositional of the stream . . . . .	23
Table 2.2 Compositional and Properties . . . . .	24
Table 2.3 Properties of the alcohol . . . . .	24
Table 2.4 Constraints on the final product . . . . .	24
Table 2.5 Contribution of Each Product . . . . .	25
Table 2.6 Fuel Testing Matrix . . . . .	28

## LIST OF FIGURES

Figure 1	Reactor used for elevated temperature . . . . .	11
Figure 2	Graph of carbon and nitrogen . . . . .	12
Figure 2.1	Schematic of the network . . . . .	30
Figure 2.2	Results for Case 1 for a refinery . . . . .	31
Figure 2.3	Results for Case 2 for a refinery . . . . .	32
Figure 2.4	Energy Overall Efficiency & Distributions . . . . .	33
Figure 2.5	Energy Production and Consumption . . . . .	34
Figure 2.6	Formaldehyde and Methanol Sampling . . . . .	35
Figure 2.7	Schematic of the Bag Sampling and Evacuation . . . . .	36

## Executive Summary

The WVU plug-flow microreactor system is now complete. Screening runs with this system will commence. Computer control is being installed in the second WVU unit. Additional hardware has been suggested for this system so that it can be used either to screen additional catalysts or to obtain kinetic data on selected catalyst samples. This may require some reallocation of equipment and personnel resources. At Union Carbide, the reactor units are to be modified to prevent secondary reactions expected either by catalysis with the reactor walls or from impurities in the reactant stream.

Synthetic preparations and characterizations of molybdenum-based sulfide and nitride catalysts are ongoing. The apparatus used for high-temperature reactions between metal carbonyls and hydrogen sulfide or ammonia was modified to allow the formation of mixed-metal sulfides.

Modelling studies are continuing satisfactorily. A more-detailed model of the reaction kinetics, to account for individual alcohols rather than a lumped higher-alcohol, has been inserted into the model of a plug-flow reactor. Results are being compared to experiments reported in the literature.

A solution methodology to maximize the profitability of alcohol production, separation and blending has been developed. The temperatures, pressures, flowrates, and key component recoveries in the separation steps are the optimization variables. This methodology was tested using two scenarios. For the first case, a refinery pool of 500,000 liters/hour was used, and the alcohol added according to the constraints of Reid vapor pressure and octane number, and conforming to the standards of the DuPont waiver. For the second case, a refinery gasoline pool of 800,000 liters/hour was used with the same constraints. The first case was not profitable whereas the second case was profitable. In each case, there was unused methanol because of its high Reid vapor pressure, and no credit was taken for any of the unused methanol. In the first case, the gasoline contained less methanol than in the second case. This methodology is robust and flexible; therefore, a wide-range of processing conditions can be investigated yielding consistent and accurate results.

The probability of this process becoming economically feasible in the near future appears to be extremely small given the low return on capital investment associated with the production of alcohol from coal. If coal derived alcohols are to become alternative transportation fuels, then the capital cost associated with the process must be reduced, specifically the cost of the gasifiers, or significant changes need to be made in the composition of the mixed alcohol product. The composition of this mixed alcohol product needs to be geared toward the production of the higher alcohols.

A methodology for performing Monte Carlo studies to determine quantitatively the uncertainties relevant to future decisions to build an alcohol-fuels plant (within the context of

an energy park) is still being developed. We have refined our simulation strategy and computer programs during this quarter.

The Cooperative Fuel Research Engine (CFR) has been instrumented and updated with all the required pressure transducers and temperature thermocouples. The data acquisition system, which includes computer hardware and software programs that will monitor all the testing events, is almost complete.

## **TASK 1. REACTION STUDIES**

### **1.1 Introduction**

The objective of Task 1 is to prepare and evaluate catalysts and to develop efficient reactor systems for the selective conversion of hydrogen-lean synthesis gas to alcohol fuel extenders and octane enhancers.

Task 1 is subdivided into three separate subtasks: laboratory and equipment setup; catalysis research; and reaction engineering and modeling. Research at West Virginia University (WVU) is focused on molybdenum-based catalysts for higher alcohol synthesis (HAS). Parallel research carried out at Union Carbide Chemicals and Plastics (UCC&P) is focused on transition-metal-oxide catalysts.

### **1.2 Accomplishments, Results and Discussion**

#### **1.2.1 Laboratory Setup**

At WVU, the plug-flow microreactor system has been completed. This reactor system is completely computer controlled, except for the reactor pressure, which (still) requires manual setting. The computer monitors and controls gas and liquid flow rates, reactor furnace temperature, automatic on-line GC sampling and GC operation. The computer also monitors the reactor pressure; the sampling valve temperature; alarms for CO, H<sub>2</sub>S, the hood fan and the hood temperature; power and house air. Automatic shutdown by the computer results in setting feed rates (liquid and gas) to zero, turning off the reactor temperature, and terminating the automatic GC sampling procedure. The second reactor system is currently undergoing computer control.

For the GC analysis, test runs indicate that a Porapak-Q packed column is sufficient for product separation. The oven temperature will be ramped from -40°C to 150°C. Two detectors, one TCD and the other FID, will be used in series; the first one to determine amounts of CO, CO<sub>2</sub>, H<sub>2</sub>O, H<sub>2</sub>S, and internal standard (Ar or N<sub>2</sub>), and possibly H<sub>2</sub>, and the second one to detect hydrocarbons.

Following a DOE review in March, we are considering ways to speed up the ability to screen catalyst samples. Accordingly, we expect to purchase equipment accessories that will allow the second reactor system to be used to screen catalysts as well as to test kinetic parameters, with minimal hardware changes. This will require an increase in the workforce for this task. Some reallocation of resources is expected.

At UCC&P, we are considering options to avoid side reactions. Under a separate DOE contract, UCC&P researchers have found that stainless steel (used as a reactor tube wall) functions as a Fischer-Tropsch catalyst if not passivated by agents such as H<sub>2</sub>S. The

effect may be non-negligible when operating at temperatures greater than 325°C with a hydrogen to carbon monoxide ratio of 0.5. This undesirable catalyzing behavior would be expected on reactor walls constructed of iron or nickel. The simplest option for the tubular micro-reactor at UCC&P may be to reconfigure the piping in the oven to enable us to use copper-lined reaction tubes. Obviously, that solution is not feasible for the UCC&P Berty reactor. We are weighing the difficulty of lining the Berty reactor against the limitations of the kinetic models which would be produced if the reactors were unlined. (Copper lining is not an option for the WVU reactors, because of the presence of H<sub>2</sub>S in the reactors. However, the presence of that gas will passivate the catalytic effect of the reactor wall.)

We have also installed carbon beds to remove iron and nickel carbonyls from feed streams to avoid poisoning of the catalysts by those compounds. We hope that this will alleviate most of the carbonyl contamination problem. Additionally, we have installed molecular sieves on feed streams for the removal of water.

We continue to experience problems with our on-line GC, but we have been able to isolate some problems and make repairs. We repaired a leak in a CO line valve, replaced a leaking GC column switching valve, replaced a solenoid that failed, and repaired another valve through which air was entering the system. We need to re-run calibration gases to verify proper working order and recalculate response factors. This has been a time-consuming process, but we have made real progress that will pay off in the quality of our final results.

We have also run liquid calibration runs off-line with the expected major alcohol products. These runs were successful, with excellent linear relationships between alcohol weights and GC areas. We will identify and calibrate for other liquid products as they appear in our product mix.

### **1.2.2 Molybdenum-Based Catalyst Research**

This section focuses on preparation and physical characterization of proposed catalysts during this reporting period. Of the four approaches described in earlier reports, most of the work this quarter has been on Approach 3. Advances in all four approaches are described below.

Approach 1. High-surface-area silica and carbon support materials have been purchased for use with the soluble mixed-metal organometallic compounds proposed in this section. Each of the six organometallic compounds described in TPR9 has been synthesized or can be synthesized readily from precursors produced in our lab.

Approach 2. Pure phase HoMo<sub>6</sub>S<sub>8</sub> has been prepared in a two-step process. In the first step, a mixture of Mo, S and Ho are ground, pelletized and reacted in an evacuated fused silica tube at the appropriate stoichiometry at 700°C for 12 hours and then at 1100°C for 48 hours, then quenched in air. In the second step, the pellet is reground, pelletized and heated

in an evacuated fused silica tube at 1100°C for 48-72 hours. This second step is necessary to convert all the Mo<sub>2</sub>S<sub>3</sub> to the Chevrel phase.

Approach 3. Building on the results reported in TPR8 and 9, additional molybdenum-based sulfides, nitrides and carbides have been made using a vapor-phase-reaction technique. These materials have been characterized. The reactor used for most of these studies is shown in Figure 1.

1. The progress made during this reporting period is in three areas:

1. Surface area, compositional and XPS characterization of molybdenum sulfides prepared by the previous reactions between Mo(CO)<sub>6</sub> and H<sub>2</sub>S at temperatures ranging from 300 to 1100°C. Preparation of MoS<sub>2</sub> at 350, 400, 450, 500 and 550 °C.

2. Preparation and characterization of molybdenum nitrides and carbides by the reaction of Mo(CO)<sub>6</sub> and ammonia in a He/NH<sub>3</sub> stream or in pure ammonia, at reaction temperatures ranging from 600 to 1100 °C.

3. Thermolytic decomposition of Fe(CO)<sub>5</sub> or Mo(CO)<sub>6</sub>/Fe(CO)<sub>5</sub> vapors in H<sub>2</sub>S.

In the first of these three areas, MoS<sub>2</sub> has been prepared from a thermolytic reaction between Mo(CO)<sub>6</sub> and H<sub>2</sub>S at 300, 500, 800, 1000 and 1100°C (see TPR8, 9). The experimental details and analytical data for these compounds are given in Table I. Based on X-ray powder diffraction data, the phase does not vary with temperature above 500°C. Elemental S and MoS<sub>2</sub> are the only two identifiable phases in these compounds. From Table I, the compositional data determined by ESCA establishes an approximate S:Mo ratio of 2 for each MoS<sub>2</sub> sample evaluated. The Mo 3d and S 2p binding energies for samples prepared at 300, 500, 800 and 1100°C (HS1, HS2, HS3 and HS6) are presented in Table II. For samples HS2, HS3 and HS6, the Mo and S binding energies match those expected for MoS<sub>2</sub>. The exception is noted in HS1, in which the Mo 3d binding energies are shifted 2 eV lower. The S 2p peak in HS1 is not split, indicating a distribution of S environments, i.e., an amorphous material.

Table I also shows that the surface area of these materials varies with reaction temperature. The maximum surface area of 82 m<sup>2</sup>/g is found for HS2 (500°C), and decreases for materials prepared at higher or lower temperatures. The decrease in surface area going from 500 to 300°C correlates with a decrease in crystallinity and a low-energy shift of the Mo 3d binding energies. Scanning electron micrographs of HS1, HS2 and HS6 indicate that the material with higher surface area (HS2) is comprised of larger agglomerations of particles, but the absolute particle size and morphology cannot be determined from the micrographs.

Additional reactions between Mo(CO)<sub>6</sub> and hydrogen sulfide have been accomplished at 350, 400, 450, 500 and 550 °C to determine the temperature at which the material surface

area is optimized. The powder X-ray diffraction patterns for these materials show broad bands indicative of amorphous materials. Surface area studies will follow.

The surface area variation for materials produced from 500 to 1100°C is consistent with conventional thermal processing. Higher temperatures induce grain growth, which typically (depending on the structure) lowers the surface area. The increase in surface area between 300 and 500°C can be understood in terms of a crystallographic phase modification. Based on the X-ray powder pattern for HS1, the material is less crystalline than HS2-HS6 (MoS<sub>2</sub> produced at 500, 800, 900, 1000 and 1100°C, respectively) and could have other phases. The only elements present in the XPS survey spectrum are Mo, S, C, and O. The binding energies of the Mo 3d electrons are shifted 2 eV to lower energy. This would correspond to a lower oxidation state and/or a modified environment for Mo. The broad peaks in the X-ray powder pattern correspond to Bragg peaks in crystalline MoS<sub>2</sub>. Therefore, it is probable that small crystallites of MoS<sub>2</sub> are forming at 300°C, causing the peak broadening in the X-ray powder pattern and changing the extended molybdenum environment.

In the second area, the decomposition of Mo(CO)<sub>6</sub> in a He/NH<sub>3</sub> flow was studied at 200, 300, 400, 500, 600, 700, 800, 950 and 1100°C (HN1-HN9, respectively). The temperature variation induced three observable phase transitions: from MoN (Mo<sub>2</sub>N or Mo<sub>16</sub>N<sub>7</sub>) to Mo<sub>2</sub>C to Mo. These phase changes occur between 800 and 1100°C. Hexagonal MoN and cubic Mo<sub>2</sub>N (or Mo<sub>16</sub>N<sub>7</sub>) are present at 800°C. Hexagonal Mo<sub>2</sub>C and a mixture of hexagonal Mo<sub>2</sub>C and Mo are present at 950 and 1100°C, respectively. The compositional variation of C and N in these compounds follows the crystallographic trend (Figure 2). Two observations can be made with regard to the surface area information. Surface areas increase with increasing temperature for a given phase and a change in phase reduces the surface area. Because the surface area changes are slight, a conclusive trend cannot be established.

In these reactions, the phase transformations followed thermodynamically dictated pathways. In all carbonyl reactions, the pressure of CO was also a controlling factor. The transition from Mo<sub>2</sub>C to elemental Mo follows the thermodynamic stability of CO. At temperatures below 950-1050°C, the disproportionation of CO to MC and CO<sub>2</sub> is favored.

Transition metal nitrides are inherently unstable with respect to N<sub>2</sub> formation. In the case of MoN, thermal decomposition occurs between 850 and 950°C. The utility of this vapor approach provides for molecular mixing of the reactants, thereby minimizing diffusion limiting processes, which results in improved thermodynamic control of the reaction relative to traditional solid-gas reactions.

For Mo(CO)<sub>6</sub> decompositions in NH<sub>3</sub> alone, two significant variations were made in the experimental conditions relative to the He/NH<sub>3</sub> reactions. In addition to using only NH<sub>3</sub>, the flow rate was lowered by a factor of 8, which resulted in longer heating times (see Table III). Experiments were conducted at 700, 800, 900 and 1000°C. The temperature-induced

phase modifications were similar to those in the He/NH<sub>3</sub> reactions, with one exception. Hexagonal MoN was the only phase observed at 700 and 800°C, in contrast to the nitride mixture detected in HN6 and HN7. Both MoN and hexagonal Mo<sub>2</sub>C formed at 900°C, while hexagonal Mo<sub>2</sub>C was the only crystalline material observed at 1000°C. In Table III, the C/N compositional variation for N1-N4 correlates to a nitride-carbide phase transition. The higher concentrations of NH<sub>3</sub> and the much longer heating times for the He/NH<sub>3</sub> reactions compared to the pure NH<sub>3</sub> reactions account for the increased crystallographic purity of N1 and N2 relative to HN6 and HN7.

For the third area, the vapor-phase reactor was modified to allow addition of Fe(CO)<sub>5</sub> and/or Co(CO)<sub>3</sub>(NO) to Mo(CO)<sub>6</sub> in order to produce mixed-metal sulfides (see Figure 1). In this modified reactor, a liquid-cooled jacket was added to the intake end of the tube to facilitate higher yields and to maintain greater temperature control. Both ends of the tube have Urry-type fused silica connectors for connection to collection and intake manifolds.

Two experiments were performed with Fe(CO)<sub>5</sub>. In the first experiment, the iron carbonyl was decomposed in flowing He (660 ml/min) at 500°C. The material was isolated in a dry box and discovered to be pyrophoric. In the second experiment, the reactor illustrated in Figure 1 was used. The reaction was performed at 800°C in a flow of He/H<sub>2</sub>S (flow rate H<sub>2</sub>S: 25 ml/min; He: 650). The resulting compound was stable in air, and had a surface area of 37.3 m<sup>2</sup>/g. The Fe:Mo:S weight ratio of 20.30:34.88:42.27 was determined by Galbraith Laboratories. This ratio and the X-ray powder diffraction pattern are consistent with a mixture of MoS<sub>2</sub>, Fe<sub>1-x</sub>S and 7.3% elemental sulfur.

Approach 4. Numerous attempts have been made to recrystallize "MoHH<sub>3</sub>L" (L=pyridine, pyrrolidine) for further X-ray crystallographic studies. The most successful technique is one in which a non-polar solvent is allowed to diffuse into a dichloromethane solution of the azide, thus decreasing the solubility of the solution and inducing crystal formation. Studies are ongoing.

### 1.2.3 Transition-Metal-Oxide Catalyst Research

We expect to begin the preparation of transition-metal catalysts in April 1994.

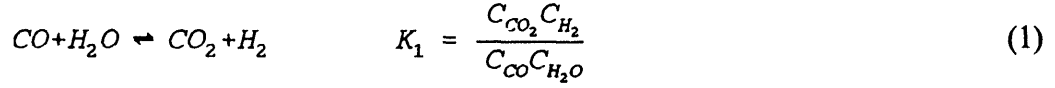
### 1.2.4 Reaction Engineering

Previously we developed computer models for three ideal reactors, namely, perfectly-mixed batch reactor (PMBR), plug-flow tubular reactor (PFTR), and continuous stirred-tank reactor (CSTR). We also developed a model for a packed-bed membrane reactor. In all these models the lumped reaction scheme of Tronconi et al. (1987) was used. This reaction scheme does not give us the concentrations of individual alcohols.

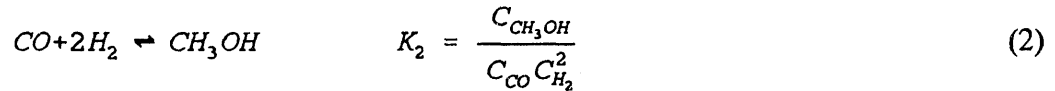
Recently, Tronconi et al. (1992) have come up with another reaction scheme which can predict the concentrations of individual alcohols and ketones. In this so-called TLGFP

scheme, two reactions are assumed to take place instantaneously at every point in the reactor.

These two reactions are the methanol synthesis reaction:



and the water gas shift reaction:



It is further assumed that hydrogenation equilibrium exists for each pair of primary alcohols and aldehydes, and of ketones and secondary alcohols.

In addition to these reactions, the TLGFP model is based on a chain-growth reaction mechanism, which is illustrated in Table IV. The chain-growth scheme takes place by three types of reactions: aldol-type condensation of carbonyl compounds; step-wise  $C_1$  additions; and reversible ketonization.

Further, both the aldol-type condensations and the step-wise  $C_1$  additions can occur via two modes: a "normal" mode and an "oxygen-retention reversal" (ORR) mode. Aldol-type condensations occurring by the ORR mode are assumed to be mainly responsible for the first C-C bond formation.

The rate expressions used for the reactor model are as follows. For aldol-type condensations and  $C_1$  additions, we have:

$$\text{Normal mode: } r_{ij} = k_{ij} K_{ad} C_i C_j \quad (3a)$$

$$\text{ORR mode: } r_{ij} = \frac{k_{ij} K_{ad} C_i C_j}{1 + K_w C_{H_2O}} \quad (3b)$$

For reversible ketonization, we have:

$$r_{ij, ket} = k_{\Gamma} K_{ad} C_1 P_{H_2} \frac{C_{ket} - \frac{C_i C_j}{P_{H_2} C_1 K_{ket, ij}}}{1 + K_w C_{H_2O}} \quad (4)$$

The rate constants  $k_j$  in the above equations depend on the nature of species taking part in a particular reaction. Tronconi et al (1992) have defined nine different parameters and have obtained the values for these parameters.

A mass balance can be written for a simple isothermal pseudohomogenous plug flow tubular reactor (PFTR):

$$\frac{dC_i}{d(1/GHSV)} = \sum_{m=1}^{N_{Ri}} \nu_{im} r_{im} \quad i=1, 43 \quad (5)$$

where  $C_i$  is the concentration of species  $i$ , GHSV is the space velocity,  $N_{Ri}$  is the number of reaction steps involving species  $i$ , and  $\nu_{im}$  is the stoichiometric coefficient of species  $i$  in the  $m$ th reaction. Using reaction rates as written in equations (3) and (4) for the reaction scheme in Table IV allows the concentrations of all species leaving the reactor to be obtained from equation (5).

A computer program TRON.FOR has been written to perform this task. The program solves 43 ordinary differential equations (ODEs) and one algebraic equation arising from the TLGFP reaction scheme (Tronconi et al., 1992) described above. These equations have been solved using LSODE, a stiff ODE solver. Preliminary results have been obtained and are being compared with the experimental data available in the literature.

### 1.3 Conclusions and Recommendations

Work on the reactor systems is proceeding at WVU and at UCC&P. Modifications have been suggested that will expedite the screening of catalysts prepared to date.

Catalyst preparation has concentrated on producing sulfides and nitrides using Approach 3 this quarter. Through a vapor-phase reaction technique,  $\text{MoS}_2$ ,  $\text{MoN}$ , and relatively pure  $\text{Mo}_2\text{C}$  can be produced. The surface area of  $\text{MoS}_2$  passes through a maximum around a processing temperature of  $500^\circ\text{C}$ . The increase in surface area between  $300$  and  $500^\circ\text{C}$  is probably due to a decreased grain size of the material produced at  $300^\circ\text{C}$  relative to the compound produced at  $500^\circ\text{C}$ .

By mixing the reactants on a molecular level prior to heating, diffusion-controlled kinetic processes are minimized and thermodynamically controlled products are produced.  $\text{MoN}$  with a surface area of  $21.1\text{m}^2/\text{g}$  can be synthesized from this vapor reaction process. The purity of  $\text{MoN}$  relative to other molybdenum nitrides can be increased by lowering the reactor flow rate and increasing the partial pressure of ammonia. Relatively pure  $\text{Mo}_2\text{C}$  can be made by varying the reactor temperature.

A mixture of  $\text{Mo}(\text{CO})_6$  and  $\text{Fe}(\text{CO})_5$  reacted with  $\text{H}_2\text{S}$  at  $800^\circ\text{C}$ , in a helium gas

stream, produces the binary sulfides,  $\text{MoS}_2$  and  $\text{Fe}_{1-x}\text{S}$ , with a surface area of  $37.3 \text{ m}^2/\text{g}$ .

Modelling efforts this quarter have concentrated on using the TLGFP model for detailed analysis of separate reaction products from a plug-flow reactor.

#### 1.4 Future Plans

Evaluation of catalyst selectivity/activity relative to higher alcohol synthesis will begin during the second quarter of 1994. This will be fast-tracked to the extent that resources are made available.

Preparation of catalyst samples will proceed using all four approaches. In Approach 1, future work will concentrate on the support of organometallic compounds, thermal decomposition, characterization and catalytic testing. In Approach 2, the surface area of the prepared Chevrel phases will be determined. In Approach 3, ternary molybdenum based sulfides, nitrides and carbides will be synthesized. The factors controlling stoichiometry, surface area and crystallographic phase will be investigated and correlated with catalytic activity and selectivity for higher alcohol synthesis. Initial studies will focus on molybdenum/iron compounds and ultimately include Co as a ternary or quaternary co-metal. With respect to Approach 4, we will focus on the characterization of the azide precursor. Support of the soluble azide compound with incremental amounts of potassium acetate, followed by thermal decomposition is expected to yield supported potassium-doped molybdenum nitride compounds.

The results of the numerical analysis using the TLGFP model in a plug-flow reactor will be tested by comparison with experimental data in the literature.

#### 1.5 References for Task 1

1. Tronconi, E., Ferlazzo, N., Forzatti, P., and Pasquon, I., Synthesis of Alcohols from Carbon oxides and Hydrogen 4. Lumped Kinetics for the Higher Alcohol Synthesis over a Zn-Cr-K oxide Catalyst, *Ind. Eng. Chem. Res.*, **26**, 2129 (1987).
2. Tronconi, E., Lietti, L., Groppi, G., Forzatti, P. and Pasquon, I., Mechanistic Kinetic Treatment of the Chain Growth Process in Higher Alcohol Synthesis over a Cs-Promoted Zn-Cr-O Catalyst, *J. Catal.*, **135**, 99 (1992).

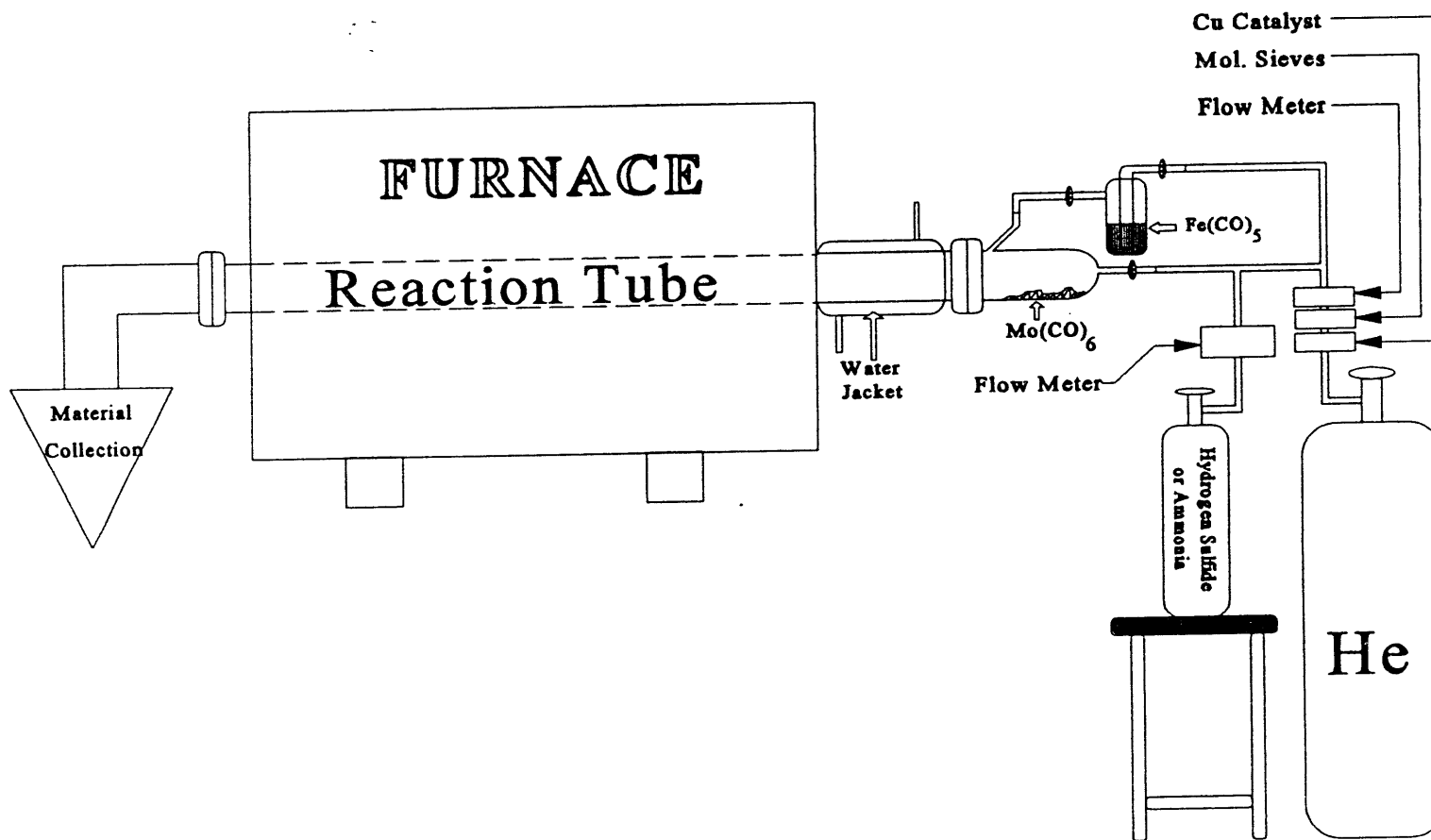


Figure 1. Reactor used for elevated temperature reaction between gaseous  $\text{Mo(CO)}_6/\text{Fe(CO)}_5$  and hydrogen sulfide in a He carrier stream.

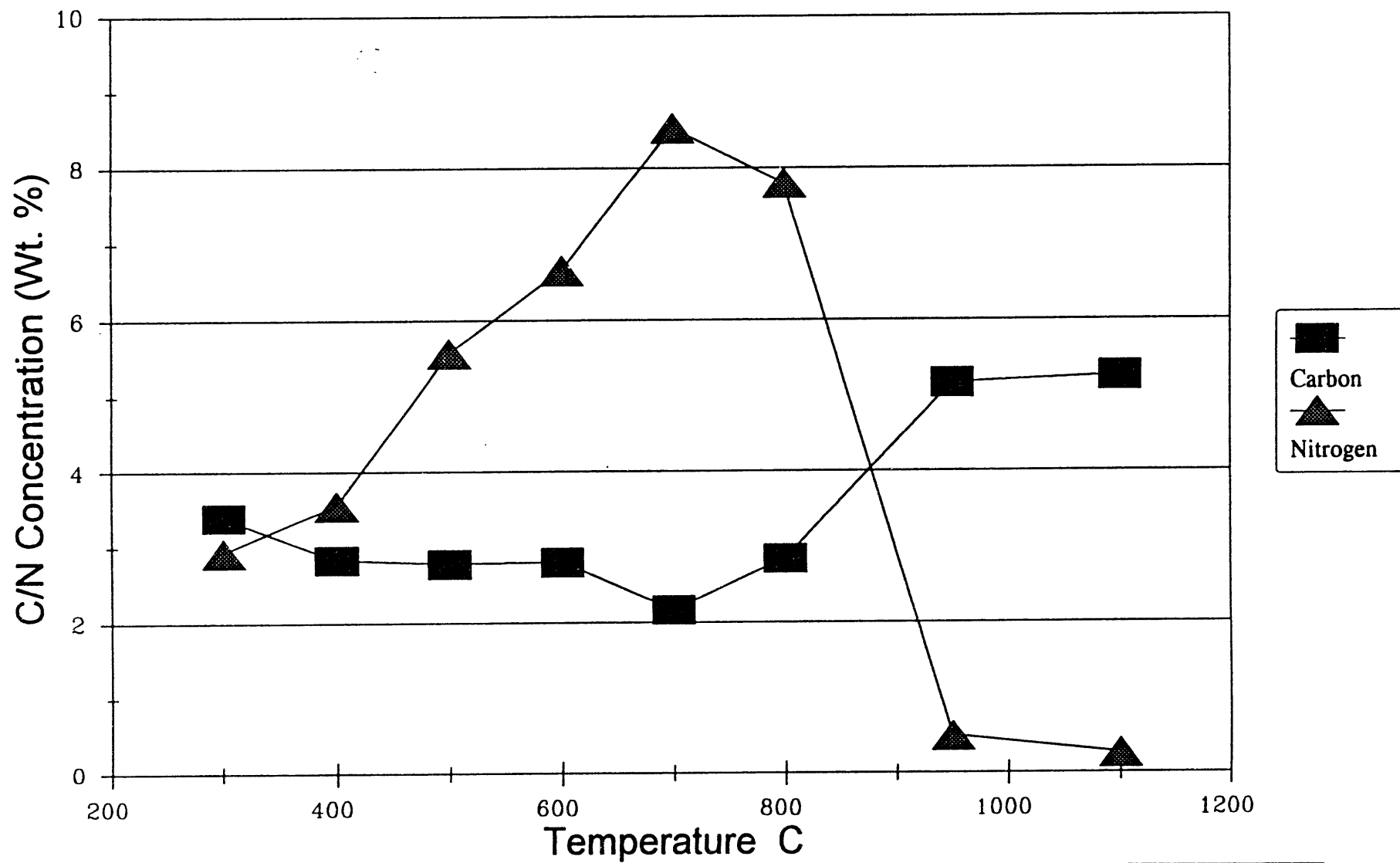


Figure 2. Graph of carbon and nitrogen concentrations in materials prepared by the reaction of hexacarbonylmolybdenm (0) and ammonia vapors, in a He carrier stream (HN2-HN9).

**Table I.** Experimental Variables and Analytical Results for MoS<sub>2</sub> Products Formed by the Reaction Between Mo(CO)<sub>6</sub> and H<sub>2</sub>S in a He Carrier Stream at Varying Temperatures.

Sample Number	Gas(es) Used	Flow Rate(s) ml/min (time) <sup>1</sup>	Temp. °C	Phase(s) Formed	Surface area, M <sup>2</sup> /g	Composition Mo, S, C, N
HS1	H <sub>2</sub> S/He	28/722 (0.3)	300	MoS <sub>2</sub> , Sulfur	18.1	C: 0.52%
HS2	H <sub>2</sub> S/He	26/635 (0.34)	500	MoS <sub>2</sub> , Sulfur	82	S/Mo = 2.34
HS3	H <sub>2</sub> S/He	26/549 (0.39)	800	MoS <sub>2</sub> , Sulfur	N/A	S/Mo = 2.11
HS4	H <sub>2</sub> S/He	26/549 (0.39)	900	MoS <sub>2</sub> , Sulfur	29.6	None
HS5	H <sub>2</sub> S/He	26/635 (0.34)	1000	MoS <sub>2</sub> , Sulfur	N/A	C: 0.42%
HS6	H <sub>2</sub> S/He	26/654 (0.39)	1100	MoS <sub>2</sub>	16.7	S/Mo=1.94; C: 0.14%

<sup>1</sup> Heating time in minutes, based on an 18 inch heating zone and the given flow rates.

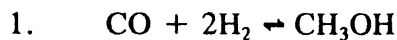
**Table II.** Mo 3d and S 2p Binding Energies for MoS<sub>2</sub> Samples Prepared From Vapor Phase Reactions Between Mo(CO)<sub>6</sub> and H<sub>2</sub>S in He.

Reference #	S 2p <sub>1/2</sub>	S 2p <sub>3/2</sub>	Mo 3d <sub>3/2</sub>	Mo 3d <sub>5/2</sub>
HS1	161.2	161	227.1	230.2
HS2	162.1	163.2	229.2	232.4
HS3	162.2	163.4	229.3	232.4
HS6	162.1	163.3	229.2	232.4

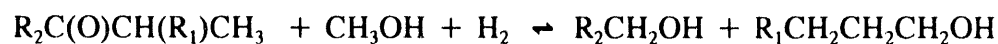
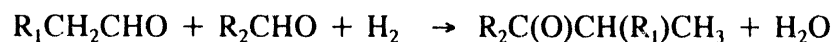
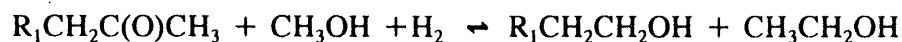
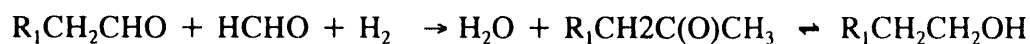
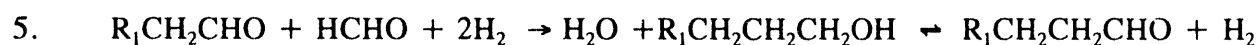
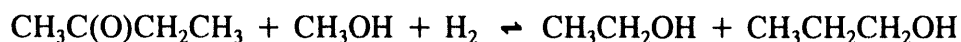
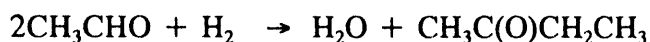
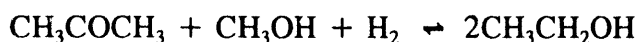
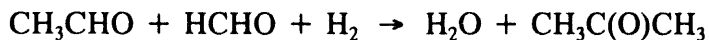
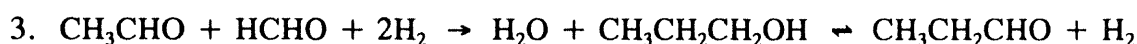
**Table III.** Experimental Variables and Analytical Results for Materials Formed by the Thermal Decomposition of  $\text{Mo}(\text{CO})_6$  in  $\text{He}/\text{NH}_3$  or  $\text{NH}_3$  Gas at Variable Temperatures.

Sample Number	Gas(es) Used	Flow Rate(s) ml/min (time) <sup>1</sup>	Temp. °C	Phase(s) Formed Powder XRD	Surface area, M <sup>2</sup> /g	Composition, Mo, S, C, N
HN1	$\text{NH}_3/\text{He}$	24/596 (0.36)	200	Broad peaks	N/A	None
HN2	$\text{NH}_3/\text{He}$	24/616 (0.35)	300	Broad peaks	14.9	C: 3.40 N: 2.94
HN3	$\text{NH}_3/\text{He}$	18/622 (0.35)	400	Broad peaks	17.1	C: 2.84 N: 3.56
HN4	$\text{NH}_3/\text{He}$	26/614 (0.35)	500	Broad Peaks	17.3	C: 2.79 N: 5.58
HN5	$\text{NH}_3/\text{He}$	26/614 (0.35)	600	Broad peaks	19	C: 2.81 N: 6.66
HN6	$\text{NH}_3/\text{He}$	65/595 (0.34)	700	$\text{MoN}$ , $\text{Mo}_2\text{N}$	20.8	C: 2.17 N: 8.54
HN7	$\text{NH}_3/\text{He}$	50/610 (0.34)	800	$\text{MoN}$ , $\text{Mo}_2\text{N}$	21.1	C: 2.85 N: 7.80
HN8	$\text{NH}_3/\text{He}$	50/610 (0.34)	950	$\text{Mo}_2\text{C}$	16.1	C: 5.18 N: 0.50
HN9	$\text{NH}_3/\text{He}$	50/610 (0.34)	1100	$\text{Mo}_2\text{C}$ , $\text{Mo}$	20.4	C: 5.28 N: 0.27
N1	$\text{NH}_3$	84 (2.7)	700	$\text{MoN}$	N/A	C: 3.61 N: 8.80
N2	$\text{NH}_3$	84 (2.7)	800	$\text{MoN}$	N/A	C: 3.42 N: 8.29
N3	$\text{NH}_3$	84 (2.7)	900	$\text{MoN}$ , $\text{Mo}_2\text{C}$	N/A	C: 5.35 N: 1.38

TABLE IV. Chain-Growth Reaction Scheme



(BY ORR C<sub>1</sub> ADDITION)



## **TASK 2. PROCESS SYNTHESIS AND EVALUATION**

### **2.1 Introduction**

A solution methodology to maximize the profitability of the alcohol production, separation and blending operations has been developed. The profitability is defined as the sum of the proceeds from the sale of the products manufactured in the plant after incorporating for the capital investment, operating expenses and the cost of raw material. The products that generate revenue are the oxygenated fuels obtained by the blending of alcohol with a pool of refinery gasoline. The raw material is the synthesis gas and the cost of the catalyst. Simulated annealing is used as the optimization technique to solve the problem of synthesis of the flowsheet and the optimization of the operating conditions. The solution to the blending problem is obtained by linear programming using the subroutine E04MBF from the NAG library of mathematical subroutines.

A simple multi-objective model base on the weighted goal programming method described in the Fourth Quarter report-1993 has been constructed and run. The results of this simulation along with the actual specification will be the emphasis of this report. The potential implications of these results will also be discussed. In addition to this discussion, two graphs illustrating the information provided in Table 2.1 of the Fourth Quarter report of 1993 are also provided for clarification.

In view of the unclear future of energy prices, governmental regulations, and process technology, we are performing Monte Carlo studies to determine quantitatively the uncertainties relevant to future decisions to build an alcohol-fuels plant (within the context of an energy park). We have refined our simulation strategy and computer programs during this quarter.

The Cooperative Fuel Research Engine (CFR) has been instrumented and updated with all the required pressure transducers and temperature thermocouples. The data acquisition system, which includes computer hardware and software programs that will monitor all the testing events, will be completed within a few weeks.

### **2.2 Accomplishments, Results and Discussion**

#### **2.2.1 Design and Optimization Of Alcohol Production, Separation and Blending**

##### **2.2.1.1 Problem Definition**

The syngas used by the reactor is being produced upstream in the plant by the gasification of coal and has an  $H_2/CO$  ratio of 1.2. The cost of syngas is \$1.994 per 1000 scf. For this problem, we assume that the syngas feed is a constant and is 8800 lbmoles at a cost of \$125 million. Table 2.1 shows the composition of the various products that exit the reactor for separation by the network of distillation columns at different values of per pass

conversion for the reactor operating at a temperature of 300°C and pressure of 2000 psig (Quarderer, 1986). The unconverted syngas is recycled, while the hydrocarbons that are manufactured are separated and used as a source of energy in the plant. Table 2.2 shows the composition and the properties of each component of the pool of gasoline available for blending with the alcohols. Table 2.3 shows the various properties of the alcohols used for this study. Table 2.4 shows the properties of the three grades of gasoline that are to be formed after blending the alcohols with the refinery pool of gasoline to manufacture the final products. The values provide the lower limits for the octane number and the upper limits for the BRVP for the oxygenated fuel. The market constraints for the demand of the various grades of gasoline are also incorporated by establishing upper limits on the amounts of the various grades that can be manufactured. The maximum amounts of Grade 2 and Grade 3 gasoline that can be produced should not exceed 25% each.

A number of oxygenated fuel blends are approved by Environmental Protection Agency (EPA). For this study, we have considered the DuPont blend which has been approved by EPA. This blend places an upper limit of 5%(v) methanol in the final product and requires a minimum of 2.5%(v) of C<sub>2</sub> to C<sub>5</sub> alcohols in the final product. The approved blend also constraints the amount of oxygen in the final fuel to 3.7%(w). The presence of water in oxygenated fuels can lead to phase separations and, therefore, the allowable limit for water is considered as 1.25%(v) in the alcohols. We also assume that the maximum amount of alcohol that can be blended with the final product is 10%(v). For the purpose of optimization we assume that our alcohol synthesis and separation facility operates 8000 hours per year. The size of the gasoline pool available is varied in the range of 500,000 to 1,100,000 liters/hour to study the effect on the topology and process conditions of the plant. The cost of the catalyst is assumed to be \$1000 /ft<sup>3</sup>. The fixed investment or the installed cost are recovered in a period of 5 years.

### **2.2.1.2 Simulated Annealing**

Simulated annealing is an algorithm for single objective multi-variable optimization problems and is based on the Monte-Carlo method for the simulation of physical systems (Metropolis, et al., 1953). Simulated annealing was introduced by Kirkpatrick, et al., (1983) by drawing an analogy between the minimization of energy achieved by annealing a physical system and the minimization of a cost function required in optimization. The algorithm for simulated annealing consists of repeatedly making a move to change the existing system configuration and accepting the move based on a mathematically derived acceptance probability while periodically reducing the annealing temperature. The algorithm is made to terminate when a specified termination condition is satisfied. In the present study, we have used the Metropolis move acceptance criterion (Metropolis, et al., 1953) with the Aarts and van Laarhoven annealing schedule and termination criterion (Aarts and van Laarhoven, 1985).

### 2.2.1.3 Solution Methodology

The separation block consists of a network of distillation column which separate the various alcohols to create appropriate blends. The total cost of the network of distillation cost is the sum of the installed and the operating cost of each column, which include the cost of the distillation column, condenser and reboiler and the cost of the hot and cold utilities. The cost of the heat exchangers which heat or cool the feed for each column to appropriate temperature along with heat exchangers which reduce the cost of the final product streams to 25°C before blending operations are also incorporated. The separation has to be done in an appropriate manner so that the blending of these fuels with the available pool of gasoline leads to the maximum profitability while incorporating a number of constraints on octane number, BRVP and oxygen content along with limits on amounts of various alcohols and water that are blended.

In this study four distinct key component separations are considered. The first set of key components are methanol and ethanol. The high Reid vapor pressure of methanol leads to a lot of methanol not being used in the alcohol blend. The second set of key components considered for separation are ethanol and propanol. This separation leads to bulk of the water present in the feed exiting as the top product with ethanol. The large amount of water present in ethanol makes it unsuitable for blending with gasoline due to the problems of phase separation. The separation of water from alcohol requires ethylene glycol as an entrainer. Therefore, the third key component considered is ethanol and water with ethylene glycol recovered as the bottom product along with water. The fourth set of key components separated are water and ethylene glycol, with the ethylene glycol being recycled. The approved blend of alcohol fuels which we have considered for this problem places a constraint on the minimum amount of higher alcohols ( $C_2$  and above) which have to be blended. Due to the relatively smaller amounts of propanol, butanol and pentanol present in our feed, the heaviest product consists of a mixture of these three alcohols. As no specific requirements are stated for the individual amounts of higher alcohols, we do not perceive any advantage in separating them into pure products.

A number of variables have an effect on the installed and operating expense of each distillation column. For each column, the degree of recovery of the light and the heavy key components, pressure and pressure drop in the column, temperature of the feed stream and the composition of the feed stream are considered as explicit variables. The flowrate can be varied by changing the split ratios, thereby changing the flow through the bypass or the distillation column and effecting the cost of the network. However, the blending problem is effected only by the split ratios or the degree of recovery of the key components as changes in only these variables effect the flowrate of the output streams.

Figure 2.1 shows the general network of distillation column. It can be observed from the figure that there are nine streams containing alcohols in various proportions that exit the network. The ethylene glycol streams are recycled. It should be noted that the final solution may or may not have a finite flowrate through the various streams. A zero flowrate through

a feed stream entering a column leads to that column not being used.

The data required for generating a suitable cost model are generated by performing a number of simulations for each distillation column in the network. Each column uses a total condenser and a partial reboiler and the products exiting the column are liquids. In this study, we generate costs for the column using five different number of stages so as to identify the appropriate lowest cost. The pressure and pressure drop in the column, temperature of the feed stream and degree of key component recoveries are allowed to vary. The cost data for each column is generated for 40 different cases and regressed over a suitable equation. The model can be expressed as

$$C = a_0 + (a_1 + a_2 r^{lk} + a_3 r^{hk} + \sum_{i \in I} b_i x_i) (1.0 + p_t)^{c_1} (1.0 + p_b)^{c_2} (273.0 + t_f)^{c_3} F$$

where  $a_0$ ,  $a_1$ ,  $a_2$ ,  $a_3$ ,  $b_i$ ,  $c_1$ ,  $c_2$  and  $c_3$ , are coefficients,  $r^{lk}$  and  $r^{hk}$  are the degrees of recovery of the light component in the top product and the heavy component in the bottom product,  $x_i$  is the composition of the component  $i$  in the feed,  $p_t$  is the pressure at the top of the column,  $p_b$  is the pressure at the bottom of the column (sum of the pressure at top and pressure drop in the column),  $t_f$  is the temperature of the feed stream and  $F$  is the feed flowrate. This model predicts the costs of the column within 5% of the actual cost for the example considered in this paper for the various separations and a wide range of the variable process conditions.

The allowable range of pressure, pressure drop and temperature of the feed considered in the course of this work depends upon the process requirements and feasibility of generating columns which can perform the separation. For the problem considered the range of pressure at the top of the column is 1 to 4 atm while the range of the pressure drop is between 0 to 1 atm. The temperature of the feed stream for the columns performing the first separation of the feed stream is between 60 to 100°C. This is because the feed stream is vapor and there is no advantage in condensing it before feeding it in the first column. For all other columns the feed stream is liquid and the range of feed temperature is between 0 to 80°C. The column performing the water/ethylene glycol separation is operated at a fixed pressure and temperature of 1 atm and 120°C, respectively. This is because we want to recover the maximum amount of ethylene glycol and the operating conditions are fixed by process constraints and therefore, not optimized.

The degree of recovery of the key components for the separation of methanol/ethanol, ethanol/propanol and ethanol/water are different. The lower limit for these recoveries is such that the non-key components do not distribute themselves in the top and bottom products and are recovered either in the distillate or the bottoms. This is established by setting the limits for the recoveries of non-key components to 99% in either the distillate or the bottoms. However, for the key component recovery of ethanol/propanol water distributes in both the distillates and the bottoms. To estimate the amount of water in the top and bottom

product, a regression is done to generate a relationship that expresses the amount of water in the distillate or bottom as a function of the operating conditions and degree of recovery of the key component. It is assumed that the columns performing the separation of water/ethylene glycol operate at fixed key component recoveries so as to maximize the amount of ethylene glycol recovered. The lower and upper limits for the methanol/ethanol separations are 0.85 and 0.99, for the ethanol/propanol separations are 0.8 and 0.94 and for the ethanol/water separations are 0.9 and 0.99.

The efficient implementation of simulated annealing requires a suitable random move strategy to change the system configuration. The choice of variables that can be changed are pressure, pressure drop, temperature of feed, degree of key component separation and split ratios adjusting the flow rate through the various streams. One of the above mentioned variables is randomly selected and the current value of that variable is increased or decreased by a random amount within the specified allowable range. The random change in the randomly selected process variable can be expressed as

$$x_{i,new} = x_{i,old} \pm \phi_i \theta$$

where  $x_{i,old}$  and  $x_{i,new}$  are the values of the randomly selected variables  $i$  before and after the change,  $\phi_i$  is the maximum allowable change and  $\theta$  is a random number between 0 and 1. However, if the variable crosses the lower or the upper bounds then the variable is set equal to the bound.

It can be observed from Figure 2.1 that the blending problem solved by linear programming involves splitting each of the 9 alcohol streams and the 7 gasoline pool streams into 3 streams for blending to make the 3 grades of gasoline. Therefore, the total number of variables for the blending problem are 48 and the number of constraints are 39.

#### 2.2.1.4 Results

The first set of results presented is for the case when the size of the refinery pool of gasoline is 500,000 liters/hour. For this problem, 50 moves are made at each temperature level using a  $\delta$  of 0.9 and  $\epsilon$  of 0.0001. The total number of moves made are 8250. The computation time for this problem is 165 seconds on an IBM RS/6000 workstation. The results are shown in Figure 2.2.

The net loss for this case is \$ 28.53 million. The conversion for each pass of syngas in the reactor is 55%, the maximum allowable limit. This is because the small size of the refinery pool of gasoline requires lower amounts of alcohol. At high per pass conversion, there is a lower selectivity for alcohols and the production of methanol is minimized with respect to higher alcohols. This leads to the formation of the maximum 10% blends, while not violating the allowable limits for the RVP and the oxygen content in the fuel. Out of the 500,000 liters/hour of refinery pool of gasoline 470,493 liters/hour is blended with the

alcohols. The bulk of the unused portion of the gasoline pool is n-butane that has a very high BRVP. Most of the alcohol that is not used is methanol which has a high BRVP and oxygen content. Out of a total of 58827 liters/hour of alcohol entering the separation block, 52277 liters/hour is blended with gasoline, indicating a 88.9% usage for the alcohol. The cost of the reactor is \$2.57 million and the cost of the catalyst is \$5.78 million. The cost for the four columns  $C_1$ ,  $C_2$ ,  $C_3$  and  $C_4$  are \$2.01 million, \$1.34 million, \$1.33 million and \$0.92, respectively. All the columns operate at a pressure of 1 atm at the top and bottom. The key component recoveries for the column  $C_1$  are 0.85 and 0.85, for the column  $C_2$  are 0.894 and 0.8 and for the column  $C_3$  are 0.99 and 0.99.

It should also be noted that Grade 1 of gasoline has the highest amount of methanol while Grade 3 has the smallest. This is because it is easier to accommodate methanol in a lower octane grade because a corresponding amount of low RVP fuel can be added which has sufficiently high octane number. As the pool has limited amounts of component having octane number close to 92 and low enough RVP, the addition of methanol in higher grades of gasoline is restricted. It should also be observed that the maximum amount of higher alcohols is found in the highest grade of gasoline.

The second set of results presented is for the case when the size of the refinery pool of gasoline is 800,000 liters/hour. For this problem, 50 moves are made at each temperature level using a  $\delta$  of 0.9 and  $\epsilon$  of 0.0001. The total number of moves made are 9100. The computation time for this problem is 182 seconds on an IBM RS/6000 workstation. The results are shown in Figure 2.3.

For this case, there is a net profit of \$ 14.46 million. The conversion for each pass of syngas in the reactor is 34%, far below the maximum allowable limit. This is because the refinery pool of gasoline is larger and more alcohol can be blended for the final product. The lower per pass conversion leads to a higher selectivity for alcohols. However, methanol production is higher leading to blends lower than the maximum allowable 10%. Out of the 800,000 liters/hour of refinery pool of gasoline 693,446 liters/hour is blended with the alcohols. As in the previous case, the bulk of the unused portion of the gasoline pool is n-butane that has a very high BRVP. Most of the alcohol that is not used is methanol which has a high BRVP and oxygen content. Out of a total of 75741 liters/hour of alcohol entering the separation block, 73762 liters/hour is blended with gasoline, indicating a 97.39% usage of the manufactured alcohol. The cost of the reactor is \$2.66 million and the cost of the catalyst is \$6.13 million. The cost for the four columns  $C_1$ ,  $C_2$ ,  $C_3$  and  $C_4$  are \$2.94 million, \$1.93 million, \$1.60 million and \$ 0.98, respectively. All the columns operate at a pressure of 1 atm at the top and bottom. The key component recoveries for the column  $C_1$  are 0.85 and 0.85, for the column  $C_2$  are 0.894 and 0.8 and for the column  $C_3$  are 0.99 and 0.99.

It should also be noted that Grade 1 of gasoline has the highest amount of methanol. Additionally, the amount of methanol in various grades in case 2 is higher than in various grades of case 1. This is because in blends of less than 10% it is easier to accommodate

more methanol without violating the constraints on RVP and oxygenate content. It should also be observed that the maximum amount of higher alcohols is found in the blend with the lowest amounts of methanol because this blend has used that portion of the refinery gasoline which has a lower ratio of octane number to BRVP.

## **2.2.2 Economic Analysis**

### **2.2.2.1 Overall Efficiency**

A detailed discussion of the use of overall efficiency as an evaluation technique was provided in the Fourth Quarter report-1993. This discussion suggested that base cases using natural gas are the most efficient on an overall bases. These conclusion were originally illustrated in tabular form. However, this information may be more easily interpreted in graphical form. Figures 2.4 and 2.5 are, therefore, provided for the purposes of clarification of this concept.

### **2.2.2.2 Multi-Objective Model Development**

It has been established that the multi-dimensionality of the energy park may be captured best through the incorporation of multiple objectives. These objectives may be derived following a simple set of assumptions. The first is that this facility will be owned and operated by the private sector. If the mixed alcohol product is to be produced by the private sector then it is only logical to assume that one objective would be to maximize long run profit, since this is essentially the main objective of private sector firms. It is also reasonable to assume that a second objective would be to minimize capital investment. Given the degree of capital intensity of the gasification process, these two basic objectives may be used to formulate a simple model which may later be modified by adding additional objectives as they are deemed necessary.

**Table 2.1**  
**Composition of the stream entering the network of distillation columns**

Pass Conversion	Methanol	Ethanol	Propanol	Butanol	Pentanol	Acetates	Water	Catalyst Cost	Reactor Cost
5	4735.1	890.1	34.1	0.0	0.0	65.1	284.5	7491000	3000006
10	3772.1	1106.8	125.7	0.0	0.0	59.9	262.1	7176000	2923197
15	3126.4	1182.6	175.5	23.7	0.0	55.8	243.9	6957000	2868784
20	2550.4	1241.7	217.6	22.0	18.5	51.9	226.8	6721000	2809809
25	1983.6	1313.9	226.6	40.8	34.3	48.0	210.0	6447000	2739900
30	1633.9	1290.0	235.4	57.3	48.2	44.9	196.4	6252000	2689623
35	1326.5	1297.5	265.2	53.8	45.2	42.2	184.3	6096000	2648865
40	1087.4	1242.5	269.2	67.2	56.5	39.5	172.7	5911000	2600000
45	885.9	1206.6	295.2	63.8	53.7	45.1	197.0	5851000	2584146
50	734.9	1119.6	298.5	75.6	63.6	49.8	217.8	5793000	2568663
55	633.6	1043.7	302.3	86.5	60.6	54.3	237.2	5783000	2565751

**Table 2.2**  
**Composition and Properties of the pool of gasoline**

Type of Stream	BRVP	Octane No.	% of Pool
Isomerate	20.4	90.55	5.5
Reformate	6.1	86.10	36.8
FCC	7.0	86.30	35.3
LHC	13.1	84.40	4.1
Alkylate	4.5	91.25	9.8
N-Butane	55.0	92.50	6.4
Polymers	1.0	92.10	2.1

**Table 2.3**  
**Properties of the alcohol**

Compound	BRVP	Octane No.	% Oxyg
Methanol	64.0	116.00	50.00
Ethanol	11.5	113.00	36.36
Propanol	3.0	104.00	26.67
Butanol	2.5	87.00	21.62
Pentanol	3.0	68.00	18.60

**Table 2.4**  
**Constraints on the final product**

Type of Fuel	BRVP	Octane No.	Price
Gas - 87	8.7	87.00	0.65
Gas - 89	8.7	89.00	0.69
Gas - 92	8.7	92.00	0.75

The potential contribution of each product to the corresponding objectives must be considered in the specification of the model. These contributions are assumed to be proportional to the rate of production of each product. In the current base cases, there are essentially three products, mixed alcohol, electricity, and SO<sub>x</sub> emission reduction credits. The contribution of each of these products to the attainment of each objective are listed in the Table 1 along with the goals and weights that have been established for each objective.

Factor (Objective)	Unit Contribution Product			Goal (units)	Penalty Weight
	1	2	3		
Profit	42	50	85	≥ 667 (MM \$)	2
Capital Investment	408	114	11	≤ 1000 (MM \$)	1

Product:

- 1 Mixed Alcohol Fuel
- 2 Electricity
- 3 SO<sub>x</sub> Credits

Prices:

- \$42/bbl Alcohol Fuel
- \$50/MW-hr Electricity
- \$170/ton SO<sub>x</sub> Credits

The goal assigned to the profit objective is based on break-even cost for the facility, while the capital investment goal is based on the perceived limitations derived from the rate of return on capital along with the inherent risk associated with the production of alcohol fuels. The weights associated with the relative importance of each goal were initially selected arbitrarily. A sensitivity analysis was performed later to determine the influence of the weights. In this case, the weights were found to be insignificant. Incorporating this information into the specification described in the last quarterly report and solving this problem using the simplex method yields an optimal solution which indicates that this facility should produce electric power and take advantage of the SO<sub>x</sub> emission reduction credits while keeping alcohol production to a minimum. These results are not surprising, since the production electricity provides the greatest return on capital with the exception of SO<sub>x</sub> emission reduction credits which are constrained by the sulfur content of the coal feed.

### 2.2.3 Monte Carlo Simulation of Process Uncertainties

The need for a Monte Carlo analysis, rather than the traditional linear sensitivity analysis, was reinforced by statements made at the Fall 1993 Contractors' Conference, such as those of M. Senden of Royal Dutch Shell, who indicated for example that future real reductions in the capital costs of Shell Gasifiers are unlikely to approach 25%, a figure that had been used

in another DOE project.

We have identified sets of variables that will be considered in our uncertainty analyses. They are:

- Costs of raw materials
- Prices of side products
- Regulatory requirements
- Costs of utilities (used and produced)
- Reactor output distributions
- Capital costs
- Physical property data

For each of these sets, there are several input variables into our simulation model. We are in the process of acquiring and analyzing projections and other data to determine appropriate frequency distributions for each of these input variables. Some input variables will be modeled with Gaussian distributions, others with triangular distributions or data-specific distributions. These distributions are then sampled by the Latin-Hypercube technique to develop parameter sets for simulations.

The ASPEN model developed during this project is used for the deterministic calculations, based on the input-parameter values. The potential output variables from the ASPEN model runs are many, but we are focused initially on two: energy efficiency and cost of production. The number of runs of the ASPEN model to be made is determined by statistical requirements. One such requirement is the so-called margin of error for the cumulative frequency distribution generated by the Monte Carlo simulation for the output variables. Figure 1 shows a generic example. The solid curve is the result from the Monte Carlo simulation. It shows the fraction of simulation runs that resulted in the output variable being below a specific value (the abscissa on the figure). The dashed curves show a range (known as the margin of error) that we can be 95% confident contains the "true" cumulative-frequency curve (i.e. the curve that would be obtained had we sampled all possible values of all input variables). The margin of error can be reduced by decreasing the confidence level (95% in this case) or increasing the number of simulation runs.

The second category of results that we shall obtain from the Monte Carlo simulation is that of regression-coefficient sets. Our analyses are of two general types: multidimensional linear regressions and multidimensional ranked regressions. The advantage of the latter is that nonlinearities can be accommodated. We shall study, and determine, the influences

between the uncertain input variables and the output variables. An adaptive technique will be used to refine the input/output variable structure of the simulation, similar to iterative experimental design.

Both the uncertainty results (represented by output-variable cumulative-frequency graphs) and the influence results (represented by regression coefficients) will be used to identify strategies for uncertainty reduction, as well as to identify opportunities for future research.

#### **2.2.4 Fuel Testing**

The Cooperative Fuel Research Engine (CFR) has been instrumented and updated with all the required pressure transducers and temperature thermocouples. The data acquisition system which includes computer hardware and software programs that will monitor all the testing events, will be completed by April 8, 1994. Testing events include;

1. Temperature measurements of air flowing into the engine cylinder, fuel blend, cylinder cooling water, intake manifold, and ambient temperature.
2. Pressure measurements of in-cylinder pressure, intake manifold, lubricant oil.
3. Air and fuel flow rates
4. Crank angle rotations
5. Engine performance which include power, torque, and brake specific fuel consumption (BSFC)

##### **2.2.4.1 Fuel Specifications**

The tested fuel (blend) is 10 % alcohol and 90% gasoline (Indoline) to keep maximum oxygen content at 3.7% by weight as was stated in the DuPont waiver. Blend content is up to 5% by volume methanol plus at least 2.5% by volume cosolvents such as ethanol, propanol or butanol, and corrosion inhibitor.

The test fuel matrix is shown in the following table:

Volume %					Weight % O <sub>2</sub>
C <sub>1</sub>	C <sub>2</sub>	C <sub>3</sub>	C <sub>4</sub>	C <sub>5</sub>	
2.4	6.1	1.2	0.2	0.1	3.70
2.0	6.5	1.2	0.2	0.1	3.64
1.5	7.0	1.2	0.2	0.1	3.56
1.0	7.5	1.2	0.2	0.1	3.48
0.5	8.0	1.2	0.2	0.1	3.41
0.0	8.5	1.2	0.2	0.1	3.33

#### 2.2.4.2 Exhaust Gas Emissions Sampling System

The sampling system was designed to dilute the exhaust gas emissions before routing to the Tedler bag. Sample collected in the Tedler bag will analyzed to measure concentration of regulated pollutants (CO, HC, NO<sub>x</sub>, and PM). Diagrammatic sketches of the sampling system are shown in the Figures 2.6 and 2.7.

### 2.3 Conclusions and Recommendations

A solution methodology to maximize the profitability of alcohol production, separation and blending has been developed. This methodology was tested using two scenarios. For the first case, a refinery pool of 500,000 liters/hour was used, and the alcohol added according to the constraints of Reid vapor pressure and octane number, and conforming to the standards of the DuPont waiver. For the second case, a refinery pool of 800,000 liters/hour was used with the same constraints. The first case was not profitable whereas the second case was profitable. In each case, there was unused methanol because of its high Reid vapor pressure, and no credit was taken for any of the unused methanol. In the first case, the gasoline contained less methanol than in the second case.

The probability of this process becoming economically feasible in the near future appears to be extremely small given the low return on capital investment associated with the production of alcohol from coal. If coal derived alcohols are to become alternative transportation fuels, then the capital cost associated with the process must be reduced, specifically the cost of the gasifiers, or significant changes need to be made in the composition of the mixed alcohol product. The composition of this mixed alcohol product needs to be geared toward the production of the higher alcohols.

There appear to be two options to increasing the yield of higher alcohols in the final product. First, the methanol may be separated and then recycled. Thus, it becomes essential to have a methanol tolerant catalyst. Therefore, this possibility should be investigated so that the economics may be reassessed. Secondly, a catalyst which produces significantly lower levels of methanol should also be investigated.

A methodology for performing Monte Carlo studies to determine quantitatively the uncertainties relevant to future decisions to build an alcohol-fuels plant (within the context of an energy park) is still being developed. We have refined our simulation strategy and computer programs. Both the uncertainty results (represented by output-variable cumulative-frequency graphs) and the influence results (represented by regression coefficients) will be used to identify strategies for uncertainty reduction, as well as to identify opportunities for future research.

The Cooperative Fuel Research Engine (CFR) has been instrumented and updated with all the required pressure transducers and temperature thermocouples. The data acquisition system, which includes computer hardware and software programs that will monitor all the testing events, will be completed within a few weeks.

#### 2.4 References for Task 2

Aarts E. H. L. and P. J. M. vanLaarhoven, "Statistical Cooling : A General Approach to Combinatorial Optimization Problems", *Philips Journal of Res.*, **40**, 193 (1985).

Kirkpatrick S., C.D. Gelatt Jr. and M.P. Vecchi, "Optimization by Simulated Annealing", *Science* **220**, 671 (1983).

Metropolis N., A.W. Rosenbluth, M.N. Rosenbluth, A.H. Teller, and E. Teller, "Equation of State Calculations by Fast Computing Machines", *J. Chem. Phys.*, **21**, 1087 (1953).

Quarderer G. J., "Mixed Alcohols from Synthesis Gas", *AIChE Spring National Meeting*, New Orleans, LA (1986).

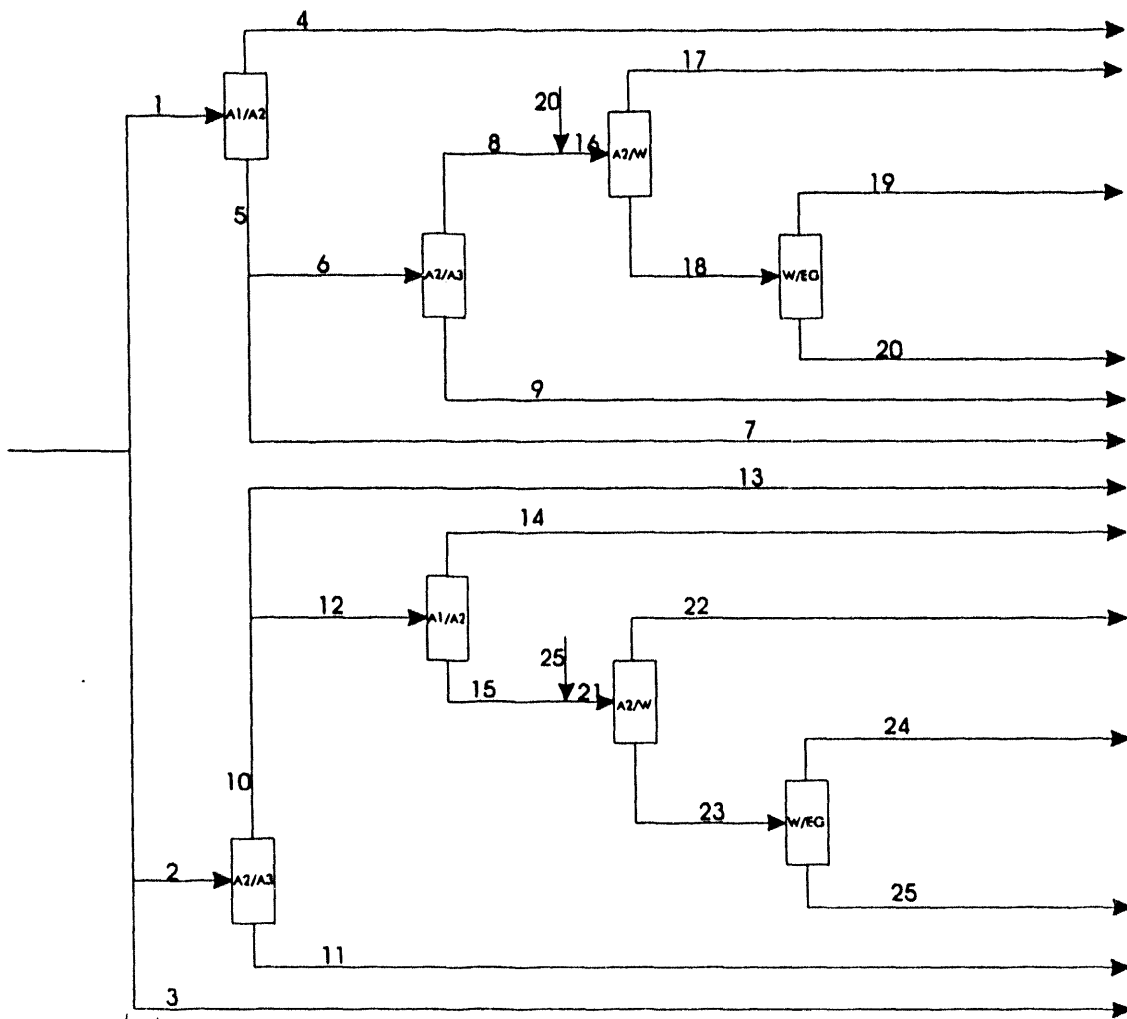
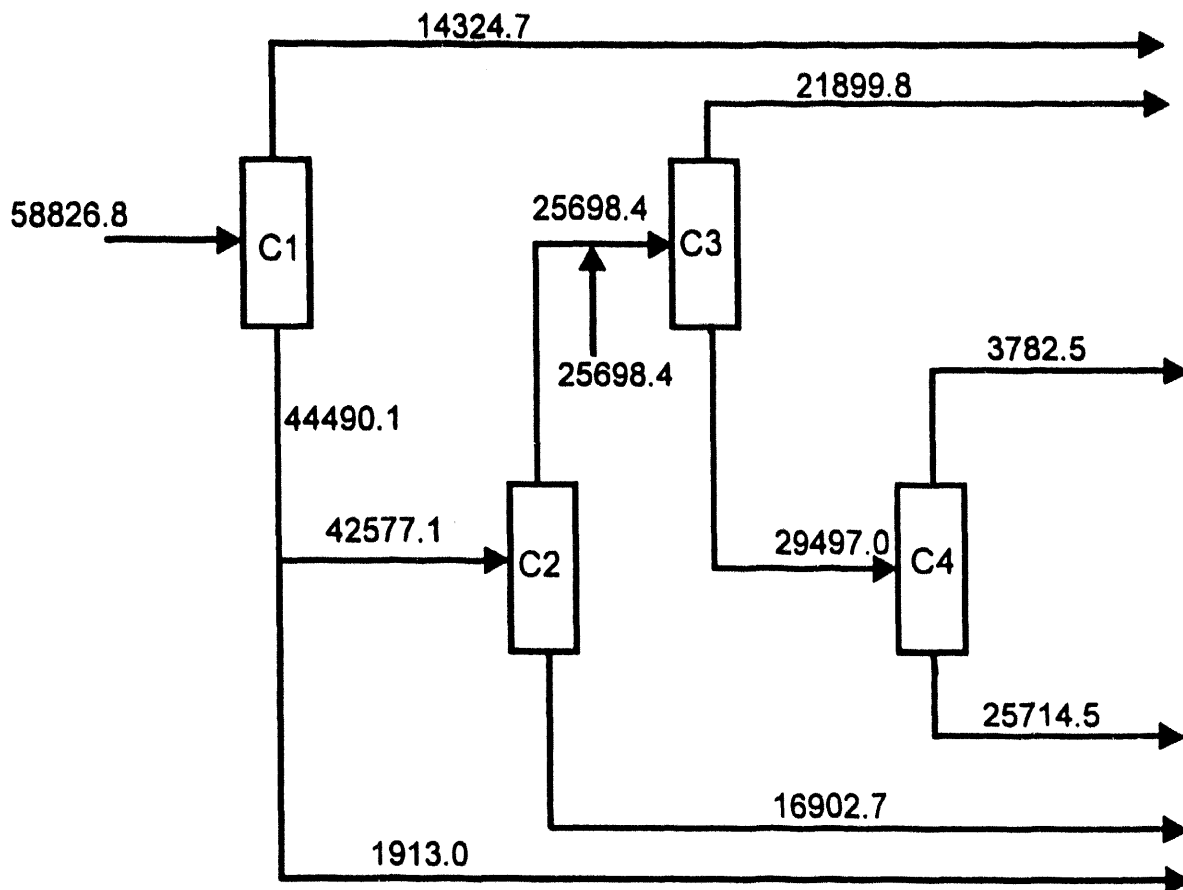
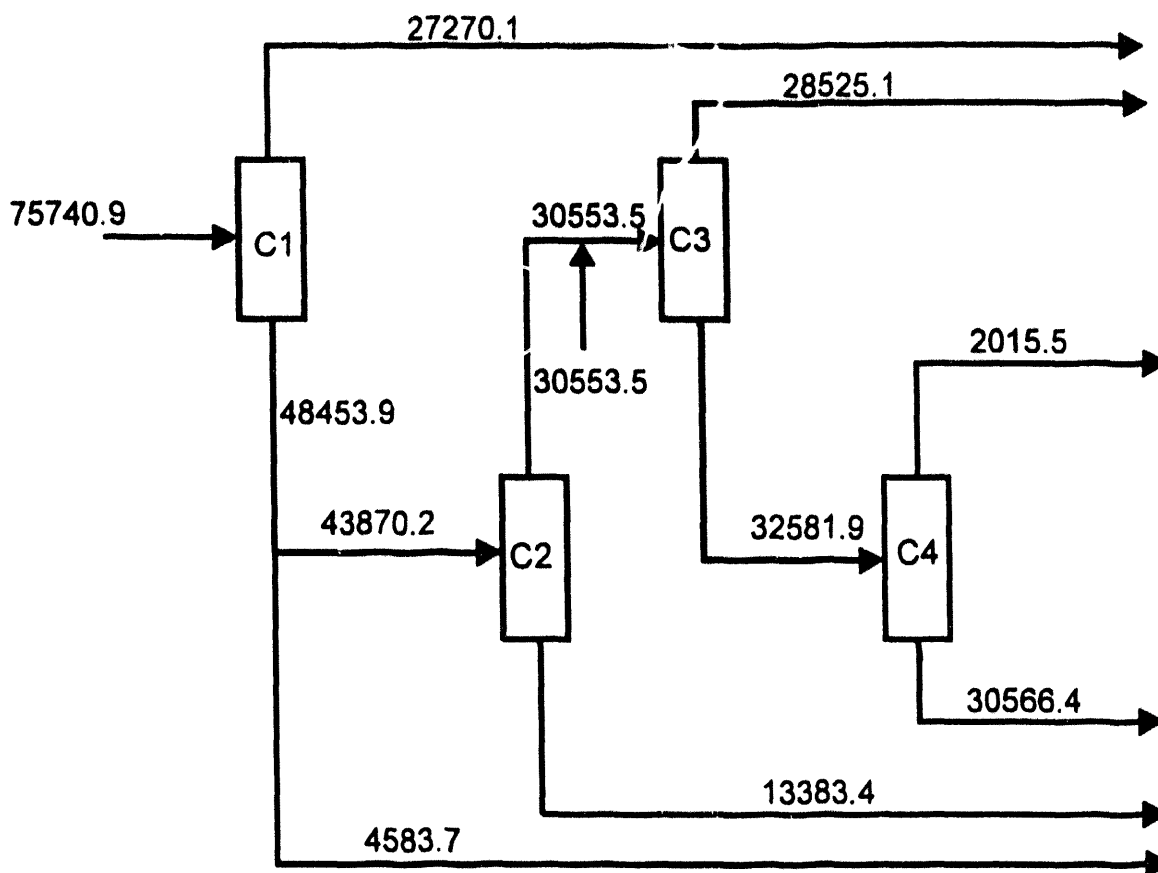


**Figure 2.1: Schematic of the network of distillation columns used to separate the alcohols**



	Grade 1	Grade 2	Grade 3
Total Flow	264920	132460	125390
Alc Flow	26492	13246	12539
BRVP	8.7	8.7	8.7
Oct. No.	87.6	89.0	92.0
% Oxyg	3.18	3.70	3.70
% Metnanol	2.22	1.80	1.39
% C <sub>2</sub> -C <sub>5</sub> Alc.	7.65	8.13	8.58
% Water	0.125	0.073	0.032
Profit	-\$28.53 million		

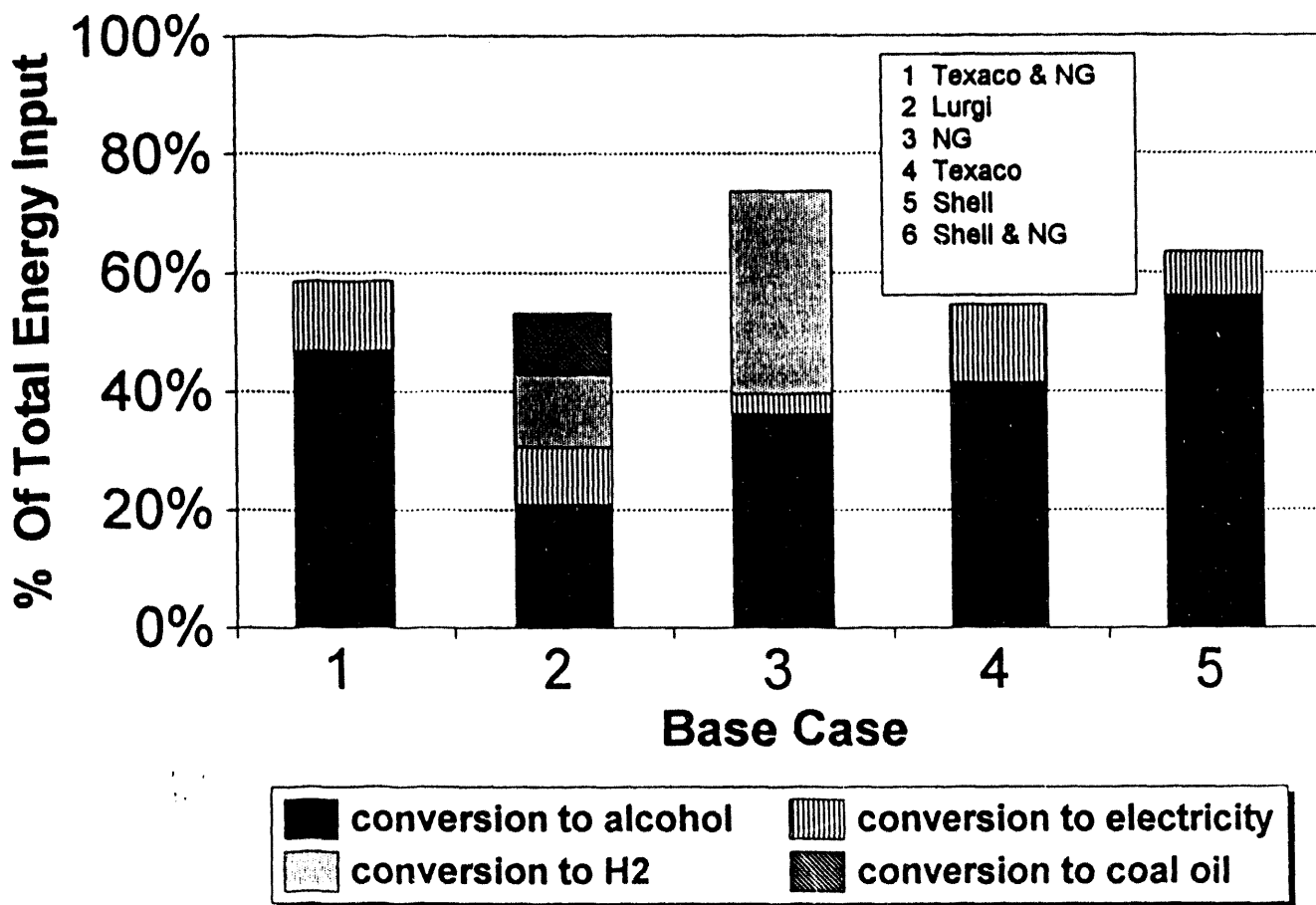
Figure 2.2: Results for Case 1 for a refinery gasoline pool of 500,000 liters/hour



	Grade 1	Grade 2	Grade 3
Total Flow	391517	195758	179933
Alc Flow	38043	18937	16782
BRVP	8.7	8.7	8.7
Oct. No	88.2	89.0	92.0
% Oxyg	3.62	3.70	3.70
% Methanol	4.25	2.02	2.96
% C <sub>2</sub> -C <sub>5</sub> Alc.	5.40	7.64	6.35
% Water	0.0065	0.007	0.011
Profit	\$14.46 million		

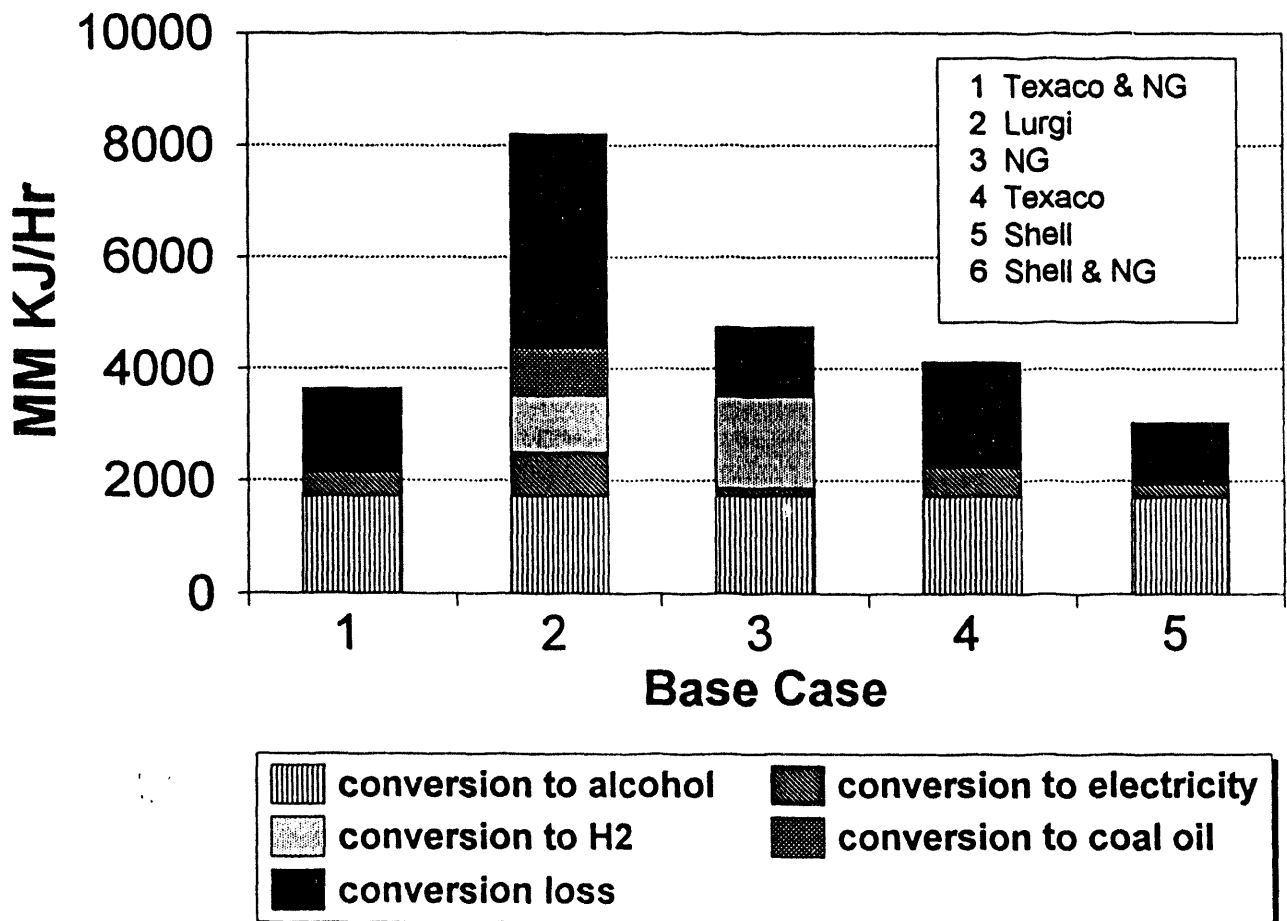
Figure 2.3: Results for Case 2 for a refinery gasoline pool of 800,000 liters/hour

**Figure 2.4**  
**Energy**  
**Overall Efficiency & Distributions**



# Figure 2.5

## Energy Production and Consumption



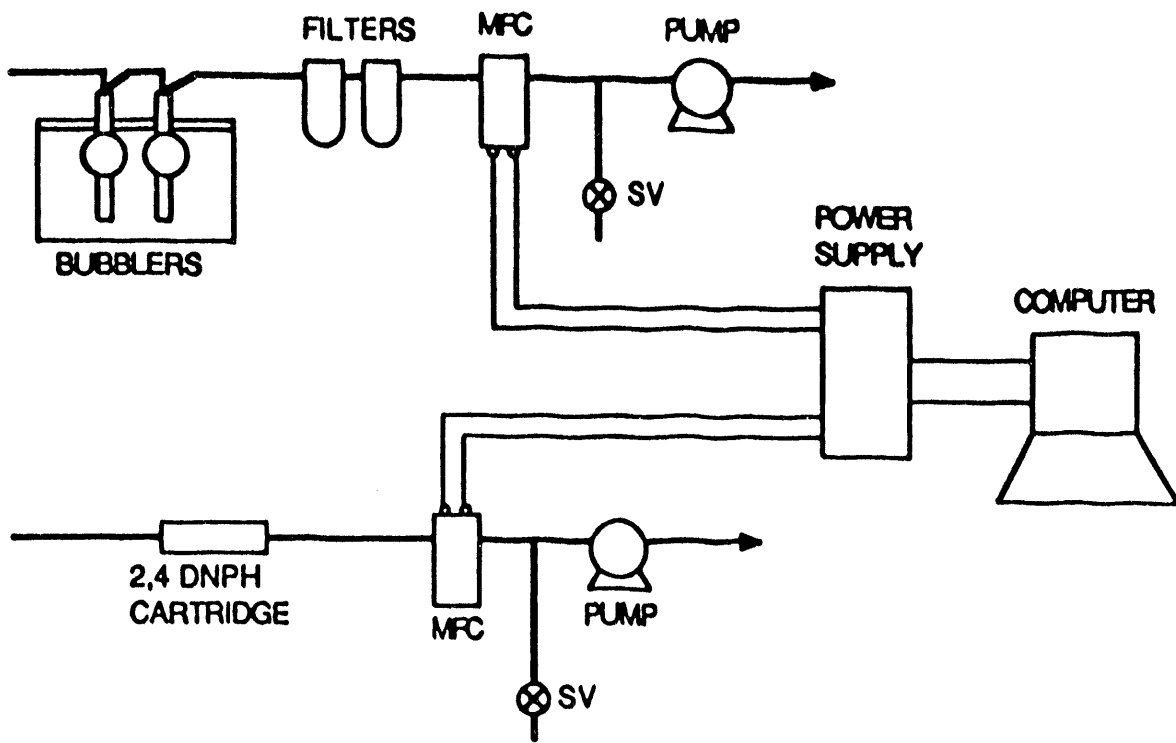
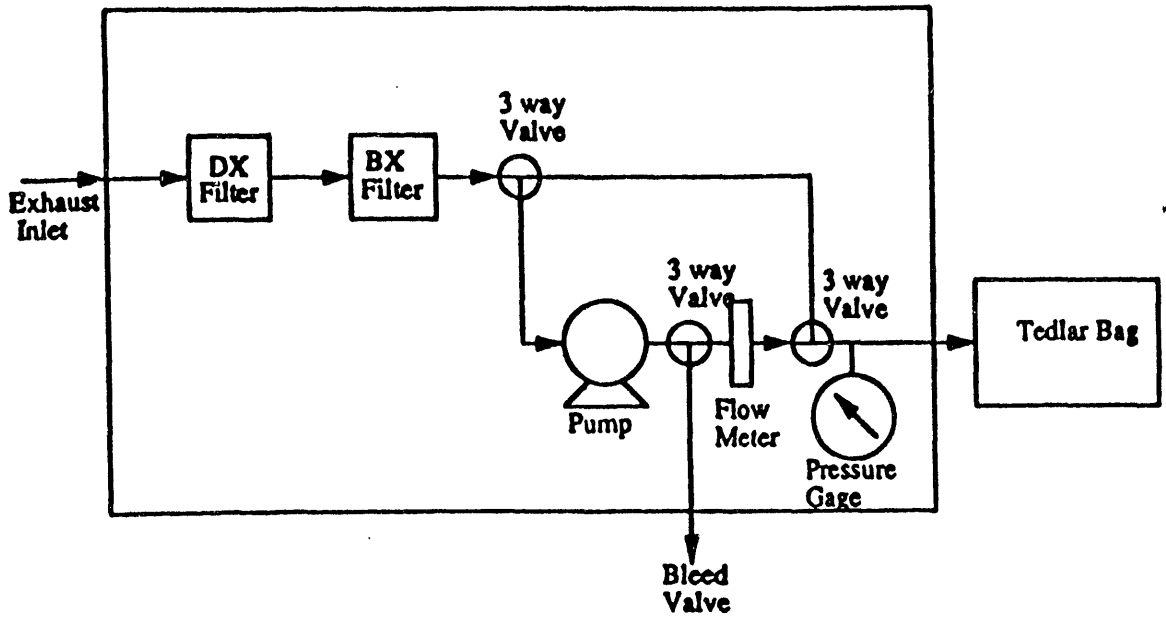
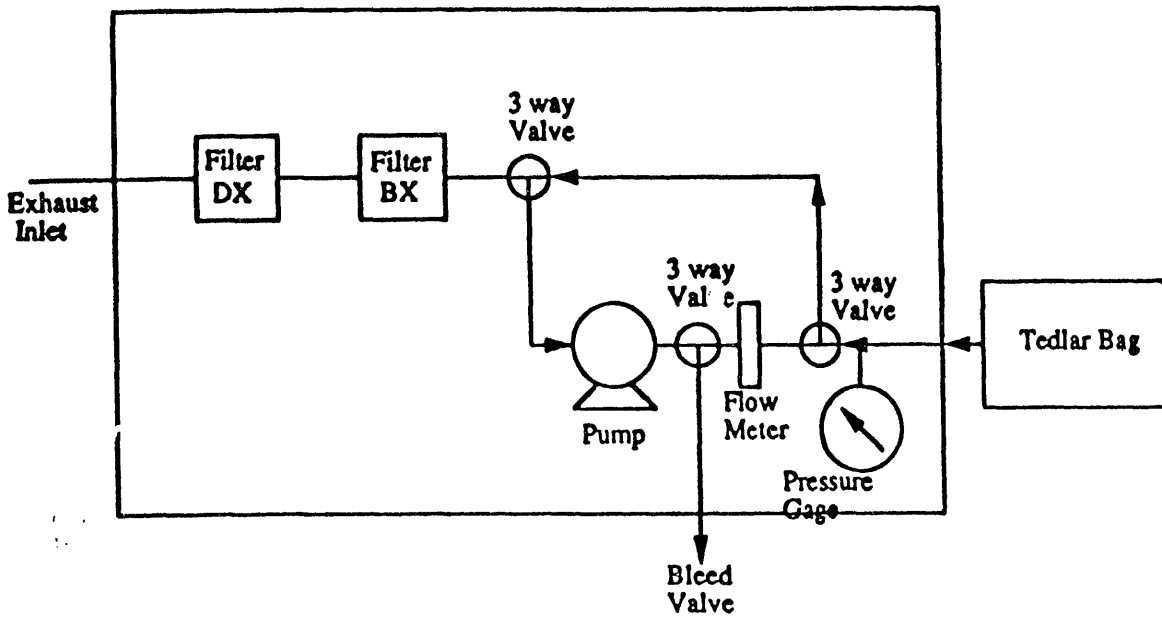


Figure 2.6: Formaldehyde and Methanol Sampling Streams



Bag Sampling



Bag Evacuation

Figure 2.7: Schematic of the Bag Sampling and Evacuation System